Available online at www.sciencedirect.com

SciVerse ScienceDirect

Ceramics International 38 (2012) 6873–6881

CERAMICS INTERNATIONAL

www.elsevier.com/locate/ceramint

Synthesis of biomorphic SiC ceramics from coir fibreboard preform

Anwesha Maity[a], Dipul Kalita[b], Nijhuma Kayal[a], Tridip Goswami[b], Omprakash Chakrabarti[a,*], Paruchuri Gangadhar Rao[b]

[a]*Central Glass and Ceramic Research Institute, CSIR, Kolkata 700032, West Bengal, India*
[b]*North East Institute of Science and Technology, CSIR, Jorhat, Assam, India*

Received 9 April 2012; accepted 28 May 2012
Available online 1 June 2012

Abstract

Coir fibre, an agricultural waste material of immense economic importance in Indian subcontinent, was used as a precursor to biomorphic SiC ceramics. Fibreboards made of coir fibres were converted to carbon templates by controlled thermal processing. Plant material precursors were characterised by analysis of molecular composition, by determination of bulk density and by scanning electron microscopy. Carbon templates were characterised by measurement of dimensional shrinkages, mass loss and bulk density and by scanning electron microscopy and XRD. The carbon templates were further subjected to infiltration with liquid Si at 1550 °C under vacuum, when spontaneous infiltration and reaction yielded composite ceramics preserving the morphology of native coir fibre derived precursors on macro and micro scale. The resulting material had a density of 2.59 g cm^{-3} and, on a microstructural scale, contained SiC and Si in addition to carbon (trace) and porosity (2 vol%). The end ceramics offered room temperature flexural strength of 116 MPa and elastic modulus of 167 GPa. Fractographic examination indicated brittle failure. The biomorphic SiC material derived from coir fibreboard precursor is likely to be suitable for use in advanced engineering applications as structural ceramics.

Keywords: Processed bio-precursor; SiSiC composite; Material property; Mechanical property

1. Introduction

For well over last two decades material scientists all over the globe have been studying synthesis of *biomorphic ceramic* materials from plant bio-structures (*plant precursors*) [1–3]. The source materials are renewable and the microstructure of the biomorphic ceramics is unique as it reflects the essential features of the cellular morphologies of the plant precursors (natural fibres, wood stems, bamboos, etc.). The properties of the final ceramics are determined by the parent plant precursors. Different precursors are used for synthesis of a variety of the biomorphic ceramic materials. Biomorphic ceramics can be oxides [4,5] or non-oxides [6,7] with majority of investigations focussed on SiC ceramics and composites [8–19]. The major advantages of the biomorphic SiC are their excellent thermal shock, corrosion and erosion resistance, adequate mechanical strength at room temperature and high temperatures, high hardness, elastic modulus at low density, permeability, anisotropic electrical properties, good machineability of the precursors and possibility of reduction of machining cost of the final materials, etc. Natural products like woods exhibit structural fluctuations which are reflected in the microstructure of the ceramics and their properties 'properties show marked changes between different kinds of woods and even different trees of same kinds of species' [20]; such variation of properties makes the biomorphic SiC unreliable in widespread applications as structural ceramics. Recently attempts are made to synthesise the biomorphic SiC using different processed precursors, such as fibreboards, papers, pressed wood powder-resin composite boards, cast bamboo pulp fibreboards, and so on [20–23]. In contrasts to natural products like woods, processed precursors are manufactured using reproducible processing techniques and their properties are reliable. Consequently the biomorphic ceramics are expected to exhibit a high extent of homogeneity of microstructure and reliability of properties. In the present

*Corresponding author. Tel.: +91 33 2473 3496; fax: +91 33 2473 0957.
E-mail address: omprakash@cgcri.res.in (O. Chakrabarti).

0272-8842/$36.00
http://dx.doi.org/10.1016/j.ceramint.2012.05.088

paper a method was described following which biomorphic SiC ceramics can be synthesised from coir fibreboard precursor. Also, microstructure, mechanical properties and results of fractographic studies were discussed.

2. Experimental

Coir is a coarse fibre that constitutes the tissues surrounding the seed of the coconut palm (*Cocos nucifera*). Coir fibres obtained from coconut trees available in the state of Assam, India, were used in the present study. The fibres contain nearly equal amount of major bio-polymers, that is cellulose and lignin (Table 1). The microstructure of coir fibre was examined under a scanning electron microscope (Model JSM 5200, JEOL, Japan). The response of the coir fibre during thermal treatment was examined by a thermal analyser (STA 490C, Netzsch-Geratebau GmbH, Germany) under flowing N_2 up to 1100 °C with a heating rate of 10 °C min^{-1}. The microstructure of the coir fibre after the thermal treatment was examined under a scanning electron microscope (SE-440, Leo-Cambridge, Cambridge, UK). Coir fibreboard was fabricated by mixing chopped fibres of length 1–1.5 cm with cellulose acetate (Loba Chemicals, India) as binder. Cellulose acetate diluted with acetone was used for homogenous mixing of fibres. The mixing was performed in a drum mixer. Subsequently the mixtures were hot pressed in a metallic mould (30 cm × 30 cm × 10 cm) at a temperature of 135 °C and a pressure of 130 kg cm^{-2}. After the pressure was released, the boards were kept in air for cooling and finally removed from the mould. The photograph of coir fibreboard is shown in Fig. 1. The coir fibreboards were cut along the length and the width into equal rectangular parts and the dimensions and weight were measured. Microstructure of the coir fibreboard was examined using scanning electron microscopy. The carbon template was synthesised by pyrolyzing the coir fibreboard sample in an electrically heated pyrolysis furnace (Steadfast International, Kolkata, India) at 800 °C under flowing nitrogen using programmed heating and cooling rates. The typical pyrolysis schedule used in the present work is shown in Fig. 2. The dimensions and the mass of the coir fibreboard carbon template were determined, XRD patterns were recorded by an X-ray diffractometer (PW1710, Philips, Holland) using Ni-filtered Cu Kα radiation of wave length $\lambda = 1.5406$ Å, and microstructure was examined under a scanning electron microscope (SEM). The biomorphic SiC was synthesised by reactive liquid silicon infiltration processing (RLSIP) technique. The coir fibreboard carbon template was suitably

Table 1
Molecular composition and other physico-chemical characteristics of coir fibre.

Major bio-polymer	Amount (% w/w)
Cellulose	43.5
Lignin	44.6
Ash content	1.8
Cold water solubility	10.5
Hot water solubility	13.9
NaOH solubility	17.0
Alcohol–benzene solubility	13.7

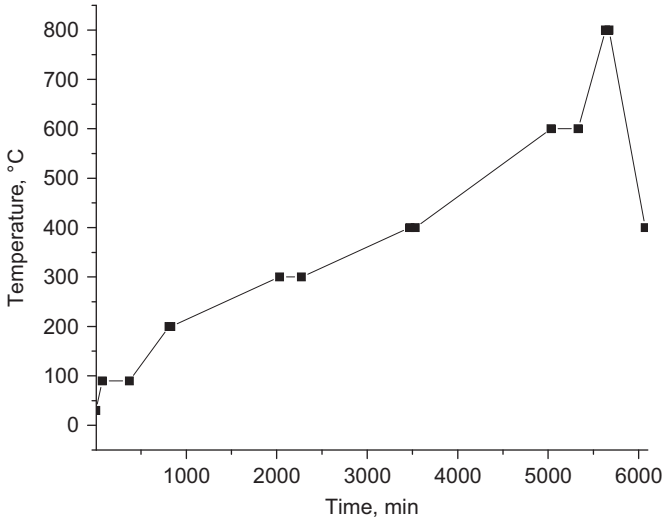

Fig. 2. Heating and cooling curves for pyrolysis of coir fibreboard samples under flowing nitrogen (gas flow rate = 20 Nl h^{-1}); samples were furnace-cooled after 400 °C.

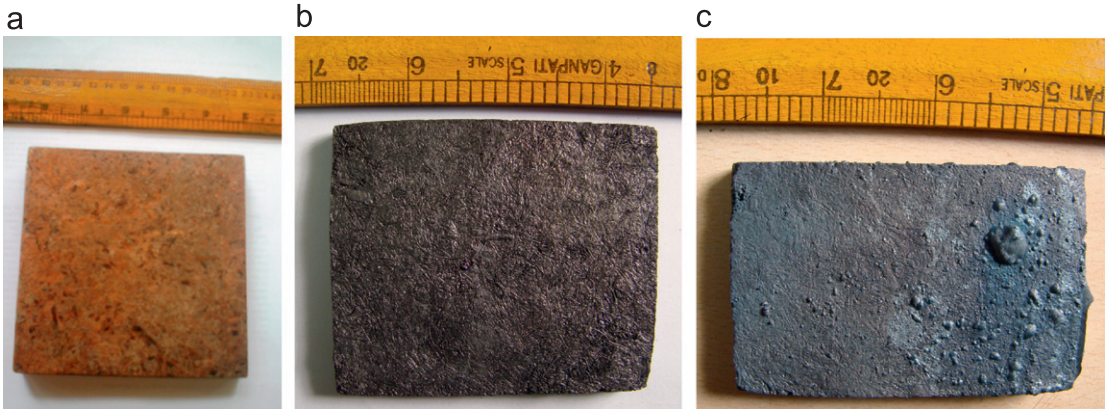

Fig. 1. Photographs showing the samples of (a) pressed coir fibreboard, (b) carbon template and (c) SiC ceramics; no major distortion in shape was noticed after carbon template making via pyrolysis and cermization via reactive liquid silicon infiltration.

contacted with liquid silicon at 1550 °C for 1 h in a graphite resistance furnace (Astro, Thermal Technologies Inc., Santa Barbara, CA, USA) when simultaneous infiltration and reaction of the liquid Si in the carbon template occurred with formation of the reaction-formed SiC ceramics. After the reaction, the furnace was cooled to the room temperature to take out the ceramic product. The dimensions of the ceramic products were measured and any un-reacted silicon adhered to the surfaces of the infiltrated specimen was removed by grinding. Open porosity and density of the ceramic product were determined by water immersion method, the crystalline phases were examined by XRD technique and microstructure was studied using scanning electron microscopy.

Room temperature flexural strength testing was done to determine the strength. A universal testing machine (Model 1123, Instron Corp., Canton, MA, USA) was used with a three point fixture. The samples were rectangular bars of 45 mm × 3.5 mm × 2.5 mm whose surfaces were ground and polished by diamond paste up to 1 μm finish and the sharp edges of the tensile surfaces were rounded off. The span and the cross head speed were 40 mm and 0.5 mm/min respectively. Young's modulus was obtained from the slope of the load–deflection curves using standard software (Instron Bluhill-2, UK). Average values of five readings of strength and elastic modulus were reported.

3. Results and discussion

3.1. Coir fibreboard fabrication

The surface of coir fibre was seen to be very rough and shallow pits were also visible. The representative SEM micrographs of coir fibre are shown in Fig. 3. The average diameter of coir fibre was found to be 275 μm. This value was well within the reported diameters of coir fibre (100–450 μm) [24]. The cross-sectional view of coir fibre (Fig. 3b) revealed cellular morphology with the cell diameter and the cell strut ranging from 2.3 to 11.8 and 1.8 to 5.1 μm respectively. Similar microstructural features of coir fibre were also reported by other authors [24]. The characteristics of coir fibreboard samples are presented in Table 2. Variation in thickness to some extent was observed. The amounts of raw fibre and binder were nearly equal in different batches, but the thickness variation reflected some degree of non-uniformity in compaction. Microstructure examination of the coir fibreboard sample revealed that the coir fibres were highly piled and their distribution was uneven (Fig. 4a). Microstructure of the sample cross-section indicated that many voids were present, their distribution was uneven and they were of moderate to large dimensions (Fig. 4b).

3.2. Coir fibreboard carbon template synthesis

The results of thermal analysis of the coir fibre are shown in Fig. 5. The thermo-gravimetric test indicated three stages of thermal degradation. There was a mass loss of around 5–6% in the first stage (at < 200 °C) which was likely due to dehydration of cellulose [25]. In the second stage 70% of mass loss occurred at 270–360 °C for decomposition of coir fibre [26]. The mass loss was accompanied with a broad exothermic peak at 350 °C probably because of recombination of degradation products like phenols and phenolic derivatives [27]. After the second stage, a slow and gradual mass loss of around 15–18% occurred up to 600 °C. An exothermic peak at 600 °C was also observed which might be due to breakdown of the –C–C– chains of polynuclear

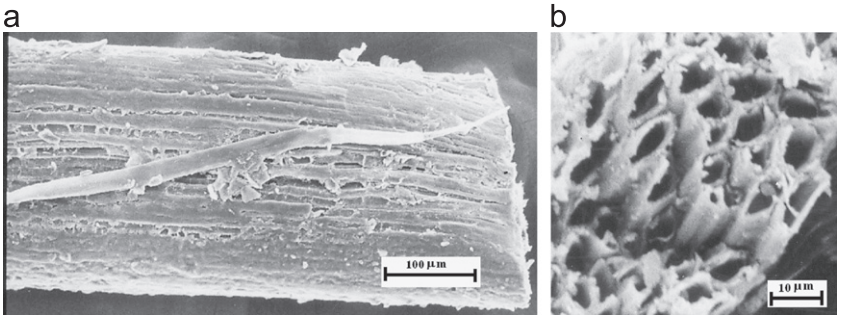

Fig. 3. SEM micrographs of the coir fibre (a) axial view and (b) cross-sectional view.

Table 2
Characteristics of pressed coir fiberboards, carbon templates and SiC ceramics.

Characteristics of pressed coir fibreboard				Characteristics of C-template					Characteristics of SiC ceramics			
Dimension (mm)			Bulk density (g cm^{-3})	Dimensional shrinkages (%)			Pyrolytic weight loss (%)	Bulk density (g cm^{-3})	Bulk density (g cm^{-3})	Porosity (vol%)	Flexural strength (MPa)	Young's modulus (GPa)
L	*W*	*T*		*L*	*W*	*T*						
129.7 ± 10.6	122.6 ± 10.7	119.3 ± 16.3	0.69 ± 0.07	23.5 ± 1.5	23.6 ± 1.8	31.9 ± 2.8	69.5 ± 1.7	0.53 ± 0.07	2.59 ± 0.04	2.04 ± 0.97	116 ± 18	167 ± 8

N.B. *L*=length, *W*=width and *T*=thickness.

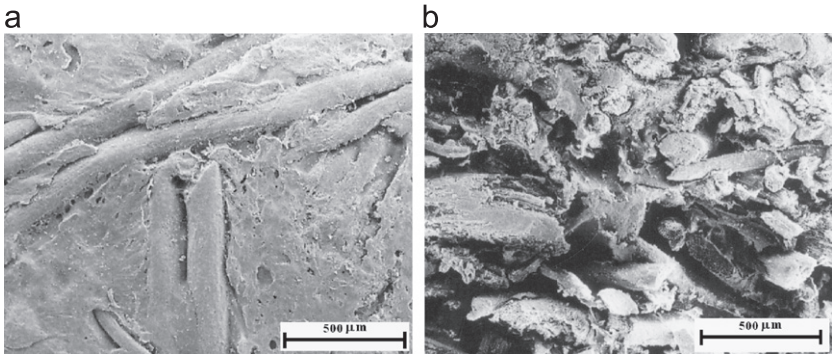

Fig. 4. SEM micrographs of coir fibreboard sample (a) longitudinal view and (b) cross-sectional view.

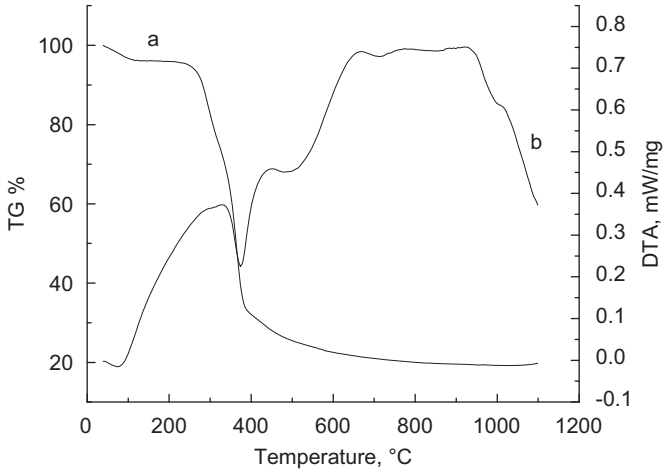

Fig. 5. Thermal analysis results of coir fibre specimen in flowing N_2 atmosphere (heating rate 10 °C min^{-1}; reference Al_2O_3) (a) TG and (b) DTA curves.

carbon structures and formation of char from cellulose and lignin [9]. During microstructure examination under a SEM, the carbon template of the coir fibre showed variation in diameter in the range of 178–333 µm with an average of 251 µm. The cross-sectional view revealed that the carbon templates were hollow. Typical microstructures of a coir fibre carbonized at 800 °C are presented in Fig. 6. The cross-section of the carbon template exhibited perfect retention of cellular morphology of the parent coir fibre. The cell diameter and the strut of the carbonized coir fibre were found to vary from 2.9 to 9.3 and 1.4 to 2.4 µm respectively. The axial view of the carbon template showed that its surface was very rough with pits and other voids occasionally filled with pyrolysis debris. After pyrolysis the coir fibreboard retained its shape with no cracks or structural disintegration evident on the surface. The photograph of the as-pyrolyzed coir fibreboard (carbon template) is shown in Fig. 1. The retention of shape was achieved by using process conditions specially designed to minimise the severity of the decomposition reactions of bio-polymers, including low process temperature and low heating and cooling rates, and large process time. The characteristics of the carbon template are summarised in Table 2. The carbon template exhibited pyrolysis shrinkages in three major directions (length, width and thickness) of 23%, 24% and 32% respectively, pyrolytic mass loss of 69%, bulk density of 0.53 g cm^{-3} and porosity of 65%. The fact that higher pyrolytic shrinkage was obtained along the thickness indicated that the green samples were not uniformly and adequately compacted along this direction. During microstructure examination retention of the fibrous morphology was seen. Pyrolyzed fibres of different diameters were seen to be unevenly stacked and the distribution of pores or void spaces was also not uniform (Fig. 7). The porous channels were seen to be interconnected. The XRD analysis results indicated the presence of broad peaks at $2\theta = 22.6^{o}$ and 44.2^{o}, as shown in Fig. 8. The peak positions are of graphitic carbon. The peak broadening indicated that the carbon sample was not fully crystalline.

3.3. Biomorphic SiC synthesis by RLSIP of coir fibreboard carbon template

The pyrolyzed coir fibres were infiltrated with silicon vapour at 1450–1550 °C for different intervals of time and the microstructure of the reaction products were examined to understand the reaction between carbon with Si and the conversion of pyrolyzed coir fibre to SiC fibre. The carbonized coir fibre after infiltration and reaction with Si vapour at 1450 °C for 10 min, exhibited perfect retention of the cellular morphology, as shown in Fig. 9(a). Energy dispersive X-ray (EDX) analysis confirmed that the struts were converted to SiC. The cellular porous morphology was partially retained after infiltration and reaction with Si vapour at 1550 °C for 10 min (Fig. 9b). When the pyrolyzed fibres were silicided at 1550 °C for 30 min a dense composite structure appeared with both the silicon and the silicon carbide detected in the microstructure of the reaction products (Fig. 9c). The carbon template of coir fibreboard was infiltrated and reacted with liquid silicon at 1550 °C for 1 h to allow complete reaction between carbon and silicon to form SiC. The Si infiltrated samples were physically inspected; no cracks or structural disintegration was noticed and retention of shape was observed (Fig. 1). The properties of the ceramic product are given in Table 2.

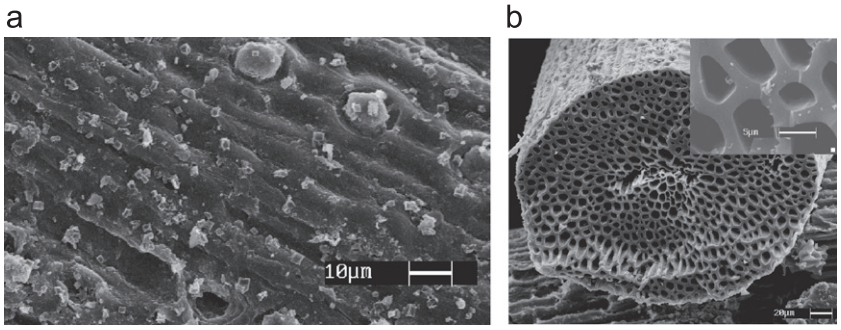

Fig. 6. Scanning electron micrographs of the carbon template of a coir fibre (a) axial view and (b) cross-sectional view showing the details of cellular morphology in the inset.

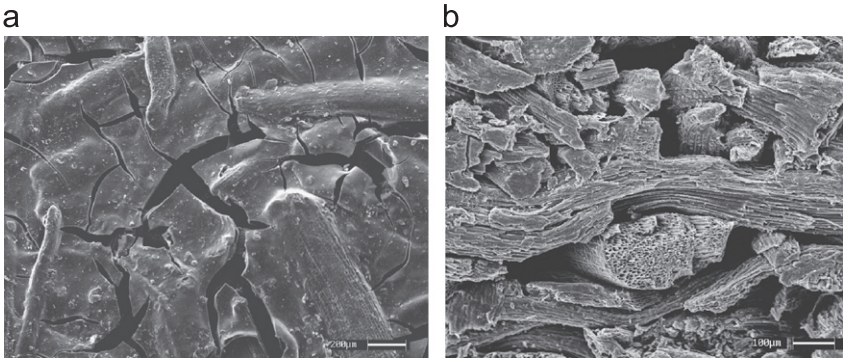

Fig. 7. SEM images of the carbon template of coir fibreboard (a) longitudinal view and (b) cross-sectional view.

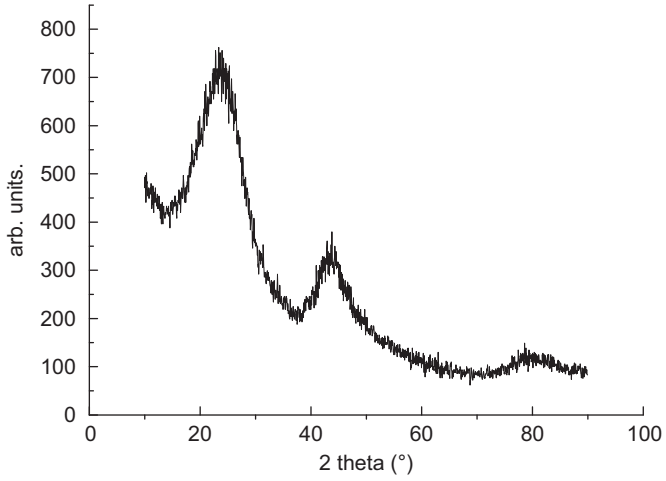

Fig. 8. XRD-profile of the carbon templates of coir fibreboard.

Marginal dimensional changes ($<1\%$) in the three major dimensions were recorded. The density and porosity of the infiltrated sample were found to be $2.59 \pm 04\ \mathrm{g\ cm^{-3}}$ and 2.04 ± 0.97 vol% respectively.

3.4. Microstructure examination

The results of XRD analysis indicated that the SiC and Si were present as the major crystalline phases in the Si infiltrated ceramic product. Typical XRD profiles are shown in Fig. 10. Microstructure examination indicated a duplex microstructure containing a bright white area (marked A) and a dark grey zone (marked B), as shown in Fig. 11(a). EDX analysis indicated these phases as SiC and Si. The fibrous morphology of the coir fibre was seen to be perfectly preserved in the SiC structure. The diameter of the SiC fibres ranged from 123 to 354 μm nearly the same range of diameter of the carbonized coir fibre. This indicated that the SiC formed preferentially in zones which were previously occupied by the carbonized coir fibres. The SiC fibres were observed to be highly piled and embedded in a matrix of solidified pool of silicon. The Si-phase was seen to be accommodated in the voids present in the carbon template. The sizes of the matrix Si-phase varied widely, indicating that the void spaces present in the carbon template were also of varying diameter. Microstructure examination also indicated the presence of fine bright white fibre-like structures of Si in the SiC fibre. The Si-phase was leached out by the action of HNO_3/HF mixture and the acid-leached samples were viewed under the microscope for examination of the microstructure in more details. The discontinuity of the SiC fibres was visible, but the microstructure clearly showed that the SiC fibres were connected, piled and randomly oriented (Fig. 11b). Microstructure examination of reaction products of fibrous carbon and liquid Si were well-documented. Pampuch et al. [28] studied the reaction of carbon fibre with liquid Si and observed that an un-reacted core of carbon fibre (of 6.2 μm original diameter and 25 vol% porosity) coexisted with small dark grey β-SiC crystals at

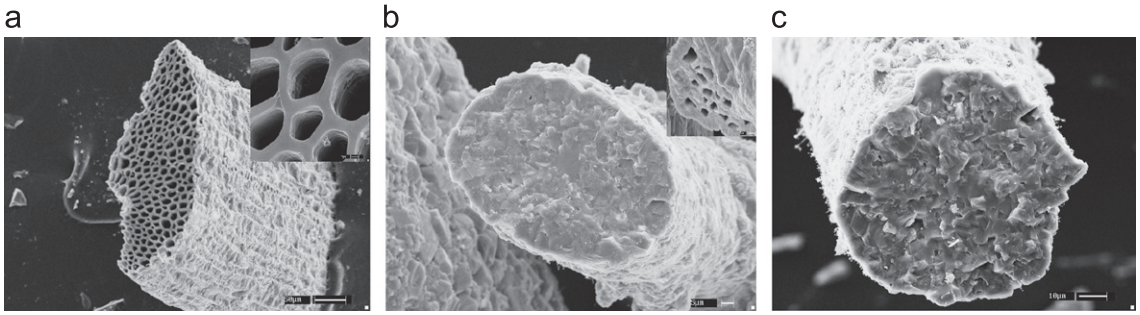

Fig. 9. SEM images of carbonized coir fibre after infiltration and reaction with Si vapour under different conditions (a) 1450 °C/10 min, (b) 1550 °C/10 min and (c) 1550 °C/30 min; the retention of cellular morphological features is shown in the insets.

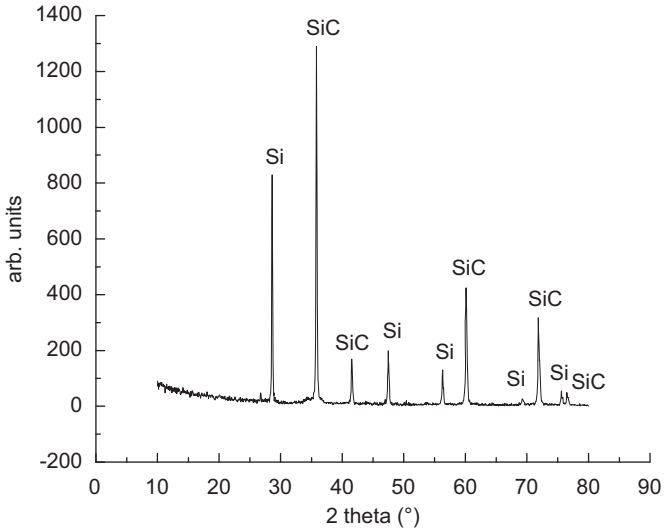

Fig. 10. XRD-profiles of Si infiltrated coir fibreboard carbon template—SiC and Si were the main crystalline phases detected.

the initial stage. The small β-SiC crystals precipitated at random in the Si matrix in localised zones previously occupied by the carbon fibres; larger β-SiC crystals were also observed at the perimeter of the zone of the small crystals. The authors also observed that the initially precipitated small β-SiC crystals grew to the dimensions of the order of 7–8 μm which led to the formation of fibrous polycrystalline β-SiC. The authors explained the preferential precipitation of the small β-SiC crystals in the vicinity of original carbon–liquid Si interface by a model based on the dissolution of carbon in Si and precipitation of SiC at its limit of solubility. The further growth of the smaller crystals to large β-SiC was explained by solution re-precipitation in liquid solution. Chiang et al. [29] also studied the mechanism of the liquid Si–carbon fibre reaction and observed a thin polycrystalline SiC product layer on the surface of the carbon fibres at the initial stage. During the subsequent stage of rapid reaction growth of larger faceted β-SiC crystals adjacent to the fibres was seen. According to the authors the volume misfit of the SiC with respect to the carbon fibre leads to spallation of sub-micron thick layer of SiC from the carbon interface increasing the solubility of carbon and subsequent precipitation of larger faceted grains. The suggested mechanism is one of the solution-reprecipitations with fine grained SiC within the fibres being the source and the sink being the large faceted crystals. Zollfrank and Sieber [30] studied the reactive silicon infiltration into microporous carbon template of beech wood leading to the formation of biomorphic SiC. During the initial stage of reaction the authors observed the simultaneous formation of a continuous nano-grained β-SiC layer at the zones previously occupied by the carbon and larger well-faceted β-SiC grains on the surface of the nano-grained SiC layer. According to the authors penetration of liquid Si into the nano-porous carbon leads to the formation of nano-grained SiC layer and simultaneous dissolution of carbon into liquid Si gives rise to nucleation and subsequent growth of larger faceted SiC crystals at the limit of carbon solubility. Afterwards the SiC reaction was found to be controlled by the diffusion of carbon through the nano-grained layer followed by dissolution in liquid Si and precipitation on the coarse SiC grains giving rise to extended grain growth. The reaction at the final stage was found to involve the dissolution of nano-grained SiC in liquid Si and re-precipitation of SiC clusters on the surface of the coarse SiC grains; the final SiC grain size was in the order of 15 μm. In the present work we removed the Si phase of the biomorphic SiC by acid etching in order to examine the morphological features of the SiC phase in more details. We observed the formation of SiC grains of two distinct morphologies—well-faceted large grains of sizes ranging approximately from 1 to 15 μm and sub-micrometre grains (Fig. 12). It appears that dissolution of carbon in Si and subsequent re-crystallisation triggered the formation of smaller SiC crystals at sites previously occupied by the carbon fibres. The larger SiC grains were probably formed by a typical process of re-crystallisation and growth of small crystals by solution-reprecipitation in liquid Si. We also observed the presence of unreacted carbon in the microstructure. It is likely that the local density of carbon varied in the carbon template. In the less dense regions carbon struts were completely reacted. The presence of unreacted carbon was likely to be related to the more dense regions where the density might exceed the critical value of 0.97 g cm^{-3} hindering the C–Si reaction [31].

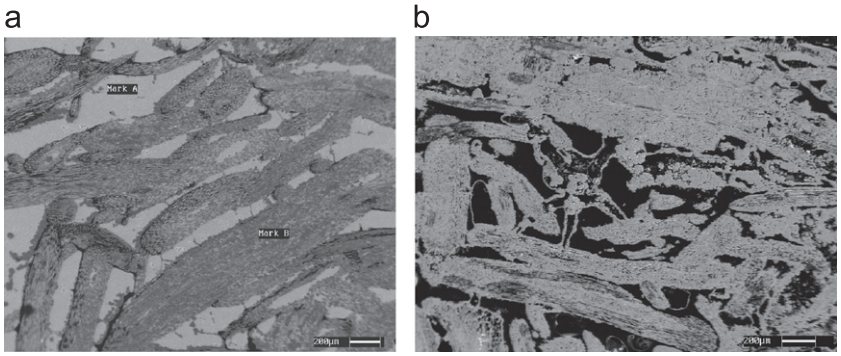

Fig. 11. SEM/BSE images of polished specimens of biomorphic SiC ceramics (a) un-etched specimen and (b) specimen etched with HNO_3/HF mixture, indicating presence of Si in the bright white zones (marked A) and SiC in the dark grey areas (marked B); Si-removed pores are clearly visible in acid-etched sample.

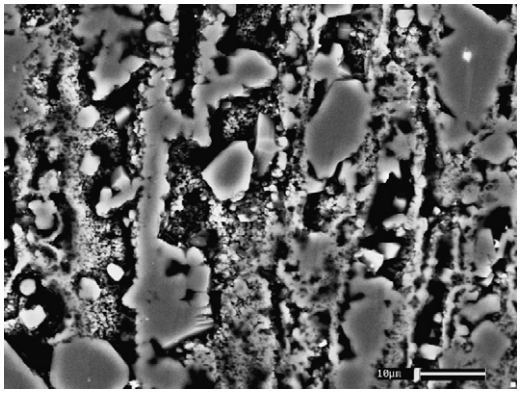

Fig. 12. Scanning electron micrograph of the surface of the biomorphic SiC ceramics after removal of Si-phase by acid etching showing polycrystalline SiC fibrous structure of two morphologies—coarse grains (1–15 μm) and sub-micrometre grains.

3.5. Mechanical characterisation

Room temperature strength testing was done to establish a reference strength of the Si infiltrated material. Five three-point fast fracture specimens were tested and had an average flexural of 116 MPa with a standard deviation of 18 MPa. The elastic modulus at room temperature measured from the slope of the load–deflection curves in the three-point bend test was found to be 167 ± 8 GPa. Many investigators reported about the mechanical properties of the biomorphic SiC ceramics synthesised from bio-precursors. Table 3 summarises the typical room temperature flexural strength and elastic modulus data of the SiC ceramics prepared from the natural and the processed precursors. In both the categories of ceramics made from natural and artificial preforms, a wide variation of mechanical properties was obtained, mainly because of the difference in material properties of the ceramics and the test parameters. The biomorphic SiC ceramics synthesised from the artificial preforms (like, wood dusts, waste cotton linters, paper laminates, medium density fibreboards, cast bamboo pulp fibreboards, etc.) exhibited a reasonably good uniformity in microstructure and reliable mechanical properties. However, the average flexural strength of 116 MPa obtained in the present work is appreciably less than 194–450 MPa three-point results of biomorphic SiC ceramics reported in Refs. [21,22,34,36,37]. The elastic modulus of 167 GPa is also less than the value of 200 GPa in Ref. [37]. But the test parameters used in the cited work must be taken into consideration while comparing the strength data. The smaller span length of 16–30 mm might be a major reason for the higher values of strength obtained by the investigators in the referred studies. Biomorphic ceramics are characterised by a microstructure that shows the presence of large areas of solidified Si which is elongated along the axial direction (growth direction of trees); silicon is also finely distributed between these large areas. The areas of elongated Si are surrounded by SiC cylindrical cores and the SiC regions are interconnected. This microstructure is a result of simultaneous infiltration and reaction of liquid Si into the porous channels of the carbon template when walls of the carbonaceous channels are converted to SiC and the remaining pores are filled with residual Si. Since Si has lower load bearing ability than SiC [38], the maximum load is carried by the interconnected SiC areas during strength testing. The microstructures of biomorphic SiC ceramics synthesised from artificial preforms are characterised by the discontinuous fibrous structure of SiC. Qiao et al. considered the lack of continuity of SiC fibres to be the reason of low strength of medium density fibreboard (MDF) derived SiC ceramics [34]. In the present study we also observed that the SiC fibres were randomly oriented and they were discontinuous. Microstructure examination showed piling of the SiC fibres; the joints between the SiC fibrous areas offered connectivity, but they were not as strong as the continuous SiC fibres. All the failed specimens were subjected to a fractographic examination under a scanning electron microscope (SEM). Typical fracture surfaces are shown in Fig. 13. The fracture surface was observed to be flat indicating brittle failure (Fig. 13a). In some samples failed at a low load porous zones localised near the surface or within the volume were also identified (Fig. 13b). The other strength limiting flaws were large grains, isolated pores and processing cracks. The results

Table 3
Typical examples of mechanical properties of biomorphic SiC ceramics synthesised from natural and processed bio-precursors determined by different investigators using different testing parameters.

Bio-precursor	SiSiC density ($g\,cm^{-3}$)	Details of the testing procedure					Room temperature mechanical property		Authors
		Bending mode	Sample size (mm)	Span (mm)	Loading rate (mm/min)	Direction	Flexural strength (MPa)	Young's modulus (GPa)	
Wood (maple)	2.50	4 pt.	5 × 6 × 60	40/20	0.5	Axial	210	275	Greil et al. [32]
						Radial tangential	132	273	
Wood (pine)	2.26	4 pt.	5 × 6 × 60	40/20	0.5	Axial	130	190	
						Radial tangential	60	200	
Wood (oak)	2.05	4 pt.	5 × 6 × 60	40/20	0.5	Axial	125	165	
						Radial tangential	40	150	
Wood (eucalyptus)	2.63	3 pt.	3 × 3 × 20	–	0.5	Axial	300	170	Presas et al. [33]
Bamboo	2.44	3 pt.	4 × 5 × 40	30	–	Axial	160	–	Qiao et al. [34]
Wood (pine)	2.62	3 pt.	4 × 5 × 40	30	–	Axial	210	–	
Wood (birch)	2.74	3 pt.	4 × 5 × 40	30	–	Axial	265	–	
Wood (coconut)	2.69	3 pt.	3.75 × 4.75 × 45	40	0.5	Axial	263	247	Chakrabarti et al. [35]
Wood (mango)	2.62	3 pt.	3.75 × 4.75 × 45	40	0.5	Axial	241	253	
Wood (jack fruit)	2.65	3 pt.	3.75 × 4.75 × 45	40	0.5	Axial	198	194	
Wood (teak)	2.52	3 pt.	3.75 × 4.75 × 45	40	0.5	Axial	180	216	
Wood (pine)	2.54	3 pt.	3.75 × 4.75 × 45	40	0.5	Axial	213	209	
Wood powder	2.90	–	–	–	–	–	227	–	Amirthan et al. [22]
	2.70	–	–	–	–	–	194	–	
Fibreboard MDF[a]	2.70	3 pt.	4 × 5 × 40	30	–	Longitudinal	185	–	Qiao et al. [34]
Paper	2.50	3 pt.	3 × 4 × 40	30	0.5	–	450	–	Yang et al. [21]
Cotton linter	–	3 pt.	3 × 4 × 40	16	0.5	–	310	–	Xue et al. [36]
Bamboo pulp fibre	2.66	3 pt.	3.5 × 2.5 × 45	40	0.5	Longitudinal	208	200	Maity et al. [37]

[a]MDF = medium density fibreboard.

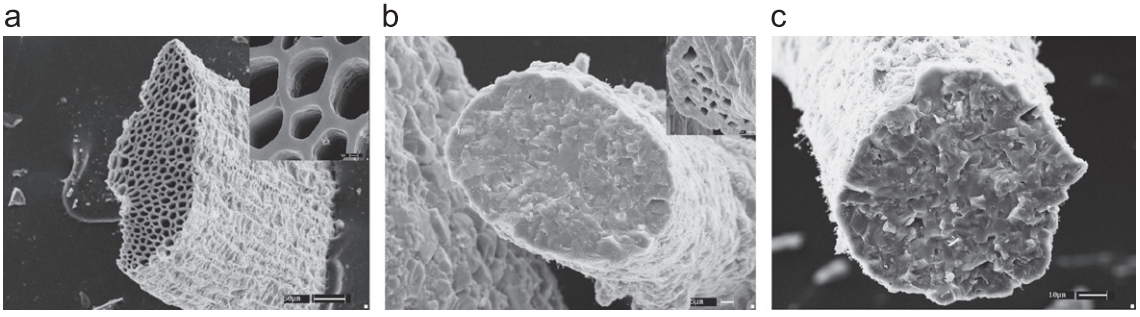

Fig. 13. Fracture surfaces of biomorphic SiC ceramic samples of varying flexural strength (a) 142 MPa and (b) 101 MPa.

of the strength testing indicated the need of further optimisation of fabrication process for coir fibreboard based biomorphic SiC ceramics.

4. Conclusions

Coir fibreboards can be converted by controlled thermal processing into carbonaceous preforms (carbon templates) maintaining the special morphological and structural features (macro and micro) that are characteristic to the biostructure. Carbon templates contain many void spaces of widely varying diameters. The carbonized fibres are discontinuous, but are interconnected and highly piled. The coir fibreboards via their carbon templates are capable of yielding SiC ceramics retaining the morphology and microstructure of the bio-precursor when infiltrated with liquid Si at 1550 °C under vacuum. A material that is ~98% dense can be prepared in a composite structure with SiC and Si as the major crystalline phases. The sample microstructure shows formation of SiC fibres that lack continuity and are embedded in a matrix of Si. The material exhibits room temperature flexural strength of 116 MPa and Young's modulus of 167 GPa. The morphology and structure of the biomorphic SiC derived from coir fibres suggest that the material is likely to be used as a structural ceramics in many advanced engineering applications.

Acknowledgement

The support of the Coir Board, Ministry of Micro, Small and Medium Enterprises, Govt. of India for carrying out the work and in granting one of the authors (AM) a fellowship (project assistant) is acknowledged with thanks.

References

[1] J.E. Mark, P.D. Calvert, Biomimetic, hybrid and in-situ composites, Materials Science and Engineering C1 (1994) 159–170.
[2] C.E. Byrne, D.C. Nagle, Cellulose derived composites—a new method for material processing, Materials Research Innovations 1 (1997) 137–144.
[3] H. Sieber, C. Hoffmann, A. Kaind, P. Greil, Biomorphic cellular ceramics, Advanced Engineering Materials 2 (3) (2000) 105–109.
[4] T. Ota, M. Imaeda, H. Takase, M. Kobayashi, N. Kinoshita, T. Hirashita, H. Miyazaki, Y. Hikichi, Porous titania ceramic prepared by mimicking silicified wood, Journal of the American Ceramic Society 83 (6) (2000) 1521–1523.
[5] J. Cao, C.R. Rambo, H. Sieber, Preparation of porous alumina ceramics by biotemplating of wood, Journal of Porous Materials 11 (2004) 163–172.
[6] M. Luo, J.Q. Gao, J.F. Yang, J.Z. Fang, W. Wang, Biomorphic silicon nitride ceramics with fibrous morphology prepared by sol infiltration and reduction–nitridation, Journal of the American Ceramic Society 90 (12) (2007) 4036–4039.
[7] C.R. Rambo, H. Sieber, L.A. Genova, Synthesis of porous biomorphic α/β Si_3N_4 composite from sea sponge, Journal of Porous Materials 15 (2008) 419–425.
[8] T. Ota, M. Takahashi, T. Hibi, M. Ozawa, S. Suzuki, Y. Hikichi, H. Suzuki, Biomimetic process for producing SiC wood, Journal of the American Ceramic Society 78 (12) (1995) 3409–3411.
[9] P. Greil, T. Lifka, A. Kaindl, Biomorphic cellular silicon carbide ceramics from wood: I. Processing and microstructure, Journal of the European Ceramic Society 18 (14) (1998) 1961–1973.
[10] D.W. Shin, S.S. Park, Y.H. Choa, K. Niihara, Silicon/silicon carbide composites fabricated by infiltration of a silicon melt into charcoal, Journal of the American Ceramic Society 82 (11) (1999) 3251–3253.
[11] M. Singh, J.A. Salem, Mechanical properties and microstructure of biomorphic silicon carbide ceramics fabricated from wood precursors, Journal of the European Ceramic Society 22 (2002) 2709–2717.
[12] F.M. Varela-Feria, J. Martinez-Fernandez, A.R. de Arellano-Lopez, M. Singh, Low density biomorphic silicon carbide: microstructure and mechanical properties, Journal of the European Ceramic Society 22 (2002) 2719–2725.
[13] A. Hofenauer, O. Treusch, F. Tröger, G. Wegener, J. Fromm, M. Gahr, J. Schmidt, W. Krenkel, Dense reaction infiltrated silicon/silicon carbide ceramics derived from wood based composites, Advanced Engineering Materials 5 (11) (2003) 794–799.
[14] J. Qian, J. Wang, Z. Jin, Preparation of biomorphic SiC ceramic by carbothermal reduction of oak wood charcoal, Materials Science and Engineering A 371 (1–2) (2004) 229–235.
[15] O.P. Chakrabarti, H.S. Maiti, R. Majumdar, Biomimetic synthesis of cellular SiC based ceramics from plant precursor, Bulletin of Materials Science 27 (2004) 467–470.
[16] A. Herzog, R. Klingner, U. Vogt, T. Graule, Wood derived porous SiC ceramics by sol infiltration and carbothermal reduction, Journal of the American Ceramic Society 87 (5) (2004) 784–793.
[17] L. Esposito, D. Sciti, A. Piancastelli, A. Bellosi, Microstructure and properties of porous β-SiC templated from soft woods, Journal of the European Ceramic Society 24 (2004) 533–540.
[18] A.I. Shelykh, B.I. Smirov, T.S. Orlova, I.A. Smirnov, A.R. de Arellano-Lopez, J. Martinez-Frenandez, F.M. Varela-Feria, Electrical and thermoelectric properties of the SiC/Si biomorphic composite at high temperatures, Physics of the Solid State 48 (2) (2006) 229–232.
[19] D. Mallick, O.P. Chakrabarti, D. Bhattacharya, M. Mukherjee, H.S. Maiti, R. Majumdar, Electrical conductivity of cellular Si/SiC ceramic composites prepared from plant precursors, Journal of Applied Physics 101 (2007) 1–7 (033707).
[20] M.A. Bautista, A.R. de Arellano-Lopez, J. Martinez-Fernandez, A. Bravo-Leon, J.M. Lopez-Cepero, Optimization of the fabrication process for medium density fiber board (MDF)-based biomimetic SiC, International Journal of Refractory Metals and Hard Materials 27 (2009) 431–437.
[21] G. Yang, Y. Liu, G. Qiao, J. Yang, H. Wang, Preparation and *R* curve properties of laminated Si/SiC ceramics from paper, Materials Science and Engineering A 492 (2008) 327–332.
[22] G. Amirthan, A. Udaykumar, V.V. Bhanu Prasad, M. Balasubramanian, Solid particle erosion studies on biomorphic Si/SiC ceramic composites, Wear 268 (1-2) (2010) 145–152.
[23] A. Maity, D. Kalita, T.K. Kayal, T. Goswami, O.P. Chakrabarti, H.S. Maiti, P.G. Rao, Synthesis of SiC ceramics from processed cellulosic bio-precursor, Ceramics International 36 (2010) 323–331.
[24] K.G. Sataynarayana, C.K.S. Pillai, K. Sukumaran, S.G.K. Pillai, P.K. Rohatgi, K. Vizayan, Structure property studies of fibers from various parts of the coconut tree, Journal of Materials Science 17 (1982) 2453–2462.
[25] J. Scheirs, G. Camino, W. Tumiatti, Overview of water evolution during thermal degradation of cellulose, European Polymer Journal 37 (2001) 933–942.
[26] G.M.A. Khan, Md.S. Alam, M. Terano, Thermal characterization of chemically treated coconut husk fibre, Indian Journal of Fibre & Textile Research 37 (2012) 20–26.
[27] H.W. Wiedemann, I. Lamprecht, Wood, Hand Book of Thermal Analysis and Calorimetry, vol. 4, 1999, p. 765 (Chapter 14).
[28] R. Pampuch, E. Walasek, J. Bialoskorski, Reaction mechanism in carbon–liquid silicon systems at elevated temperatures, Ceramics International 12 (1986) 99–106.
[29] Y.M. Chiang, R.P. Messner, C.D. Terwilliger, Reaction-formed silicon carbide, Materials Science and Engineering A 114 (1991) 63–74.
[30] C. Zollfrank, H. Sieber, Microstructure evolution and reaction mechanism of biomorphous SiSiC ceramics, Journal of the American Ceramic Society 88 (1) (2005) 51–58.
[31] O.P. Chakrabarti, L. Weisensel, H. Sieber, Reactive melt infiltration processing of biomorphic Si–Mo–C ceramics from wood, Journal of the American Ceramic Society 88 (7) (2005) 1792–1798.
[32] P. Greil, T. Lifka, A. Kaindl, Biomorphic cellular silicon carbide ceramics from wood: II. Mechanical properties, Journal of the European Ceramic Society 18 (14) (1998) 1975–1983.
[33] M. Presas, J.Y. Pastor, J. Llorca, A.R. de Arellano-Lopez, J. Martinez-Fernandez, R. Sepulveda, Microstructure and fracture properties of biomorphic SiC, International Journal of Refractory Metals and Hard Materials 24 (2006) 49–54.
[34] G. Qiao, R. Ma, N. Cai, C. Zhang, Z. Jin, Mechanical properties and microstructure of Si/SiC materials derived from native wood, Materials Science and Engineering A 323 (2002) 301–305.
[35] O.P. Chakrabarti, H.S. Maiti, R. Majumdar, Final Technical Report of the Project: Cellular SiC Ceramics from Plant Precursor for Engineering Applications, Department of Science and Technology, Government of India, No. SR/S3/ME/20/2003-SERC-ENGG, September 2008.
[36] T. Xue, Z. Jin, W. Wang, Preparation and characterization of porous SiC from waste cotton linter by liquid Si infiltration reaction, Materials Science and Engineering A 527 (2010) 7294–7298.
[37] A. Maity, D. Kalita, N. Kayal, T. Goswami, O.P. Chakrabarti, P.G. Rao, Oxidation behavior of SiC ceramics synthesised from processed cellulosic bio-precursor, Ceramics International, in press (doi: 10.1016/j.ceramint.2012.02.054).
[38] K. Sumino, Deformation behavior of silicon, Metallurgical and Materials Transactions A 30A (6) (1999) 1465–1479.